Fibers and Polymers 2015, Vol.16, No.9, 2011-2020
DOI 10.1007/s12221-015-5279-9

ISSN 1229-9197 (print version)
ISSN 1875-0052 (electronic version)

Enhanced Thermal, UV Blocking and Dye Absorptive Properties of Chitosan/poly(vinyl alcohol)/Graphene Oxide Fibers

Yujiao Wang[1,2], Mingwei Tian[1,2,3]*, Lijun Qu[1,2,3]*, Shifeng Zhu[1,2], Yaning Sun[1,2], and Guangting Han[2,3]

[1]*College of Textiles, Qingdao University, Qingdao 266071, China*
[2]*Laboratory of New Fiber Materials and Modern Textile, the Growing Base for State Key Laboratory, Qingdao University, Qingdao 266071, China*
[3]*Collaborative Innovation Center for Marine Biomass Fibers, Materials and Textiles of Shandong Province, Qingdao University, Qingdao 266071, China*

(Received April 9, 2015; Revised July 8, 2015; Accepted July 14, 2015)

Abstract: Ductile appearance, remarkable length-diameter ratio, flexible fabrication properties and featured additional functions of functional composite fibers elicit great interest in applications. In this paper, chitosan/poly(vinyl alcohol) composite fibers with different graphene oxide additive (1-7 wt.%) were spun via continuous wet-spinning route and the resultant fibers revealed improved thermal, UV blocking and dye absorptive properties. In details, the component of fibers was characterized by SEM, TEM, FTIR, XRD and the results indicated that the graphene oxide dispersed well in chitosan/ PVA matrix and the hydrogen bond was occurred between these components. As expected, the highest graphene oxide content case (7 wt.% GO) possessed the extraordinary UV blocking property as its UPF value reached to 500 arising from UPF=8.11 of 0 wt.% GO case. However, the composite fiber with 1 wt.% GO, rather than 7 wt.% GO, expressed the remarkable thermal stability and dye absorptive property, and the dye absorptive property of 1 wt.% GO showed the highest absorptive capacity of 407 mg/g among all the resultant fibers.

Keywords: Graphene oxide, Fibers, UV blocking, Dye abosorptivity

Introduction

Graphene oxide (GO) prepared from natural graphite has unique two-dimensional sheet structure and some attractive properties, such as mechanical properties [1-4], UV blocking [5], thermostability [6-8], hydrophilic [4,9] and so on. The existence of abundant oxygen-containing groups, including hydroxyl, epoxy and carbonyl groups [10], provides the possibility for synthesizing various functional materials.

Polymer materials with graphene oxide have attracted a great deal of attention in recent years. As a functional additive, graphene oxide could enhance and improve physicochemical properties of polymer matrix at low content, such as PP [11-14], PE [15,16], PVC [17,18], PMMA [19], PU [20,21], cellulose [22], etc.

Chitosan, well known to consist of poly(1,4-β-D-glucopyranosamine), is the N-deacetylated polysaccharide from chitin. As a green adsorbent, chitosan possesses many distinctive properties, such as biocompatibility, biodegradability, antibacterial property, and so on. Chitosan/graphene oxide composites have attracted increasing interests in wide fields. For instance, Han *et al*. and Yang *et al*. [23,24] prepared well-dispersed chitosan (CS)/graphene oxide composites in order to enhance mechanical strength respectively. Furthermore, since by containing various chelating groups, chitosan can effectively remove dye molecules from contaminated water [25]. So some research focuses on dye absorption, for example, CS/GO composite was effective adsorbents toward methylene blue, Au (III) and Pd (II) [26-28]. Moreover, a GO/CS hydrogel was demonstrated as a new type of eco-friendly and potential absorbent for water pollution resulting from its large specific surface area, the maximal adsorption capacities towards cationic MB and anionic Eosin Y were both higher than 300 mg/g [29]. However, its application was restricted because of high cost. So it is a burning problem to seek an alternative substance which is asked to be able to blend with graphene oxide, cheap and had no effect on properties.

Poly(vinyl alcohol) (PVA), as a nontoxic synthetic polymer, has been considered as a widely used matrix, due to excellent water solubility, heat stability, adhesiveness and fiber forming [30,31]. And it contains a large amount of hydroxyl groups in the molecular structure [30,31]. Medically, Bai *et al.* prepared the GO/PVA hydrogels that suggested pH-induced gel-sol transition used for loading and selectively releasing drugs at physiological pH [32]. More, Kim *et al.* considered PVA/GO oxide composite film as transparent and high gas barrier films [33]. But above all, PVA was an excellent matrix material without doubt.

In this paper, CS/PVA were chosen and mixed homogenously with different contents of GO to spin functional blend fibers by wet-spinning route, which was found that ethanol effectively acted as coagulation bath. As a result, CS/PVA/GO fibers expressed excellent anti-ultraviolet capability, adsorbability and thermal property.

*Corresponding author: tmw0303@126.com
*Corresponding author: profqu@126.com

Experimental

Materials

Poly(vinyl alcohol), (M_w=77,000, 97 % hydrolyzed) was supplied by Tianjin BASF chemical Co., Ltd., China. Chitosan (degree of deacetylation, 93 %) was purchased from Jifa Group Co., Ltd., China. Alcohol (w%≥99.7 %) was obtained by Tianjin Fuyu chemical Co., Ltd., China. Graphite powder (nature flake graphite, sized at 30 μm) was purchased from Qingdao Huatai Tech Co., Ltd., China. Other reagents were commercially available and of analytical reagent grade. All chemicals and solvents were used as received.

Preparation of Water-soluble CS/PVA/GO Solution

Graphene oxide was prepared from graphite powder by a modified Hummers method as our previous Ref. [34,35]. 10 g of graphite powder was added to 60 m*l* of concentrated sulfuric acid at the temperature lower than 20 °C. And 12 g of potassium persulfate and 12 g of phosphorus pentoxide was added slowly under constant strring. Then the reaction system was transferred to an 80 °C water bath for 8 h. Then the resultant solution was poured into 3000 m*l* of distilled water and setting for 8 h. After taking the lower sediment and drying at 90 °C, 10 g of sediment, 250 m*l* of concentrated sulfuric acid and 30 g of potassium permanganate were mixed and stirred for 2 h at 35°C. And stop adding dropwise 30 % hydrogen peroxide until the solution turned to bright yellow. The bright yellow liquid was washed once with 2500 m*l* of 10 % hydrochloric acid and two times with 3000 m*l* distilled water. Finally, 4.4 mg/m*l* graphene oxide dispersion (GO) was fabricated through two runs of centrifugation at the speed of 8000 r/min for 3 minutes and one runs of centrifugation at the speed of 5000 r/min for 5 minutes.

A series of CS/PVA/GO were prepared with GO ranging from 0 wt% to 1 wt%, 3 wt%, 5 wt% and 7 wt%. In a typical procedure (shown in Figure 1) for preparing CS/PVA/GO with 7 wt%, 1 g CS was added to 50 m*l* GO dispersion (4.4 mg/m*l*) with acetic acid under vigorous agitation for 10h. Successively, 5 g PVA was added to 50 m*l* de-ionized water in a round-bottom flask. The solution was transferred to an 85 °C water bath until PVA was completely dissolved,

Figure 1. The prepared process of water-soluble CS/PVA/GO solution and continuous CS/PVA/GO composite fibers by wet-spinning assembly.

forming a PVA aqueous solution. Finally, the PVA aqueous solution blended with CS/GO dispersion for stirring for 2 h. The GO concentration of the final solution was determined by the volume of adding GO, which was altered by 0 wt%, 1 wt%, 3 wt%, 5 wt% and 7 wt%.

Preparation of Continuous CS/PVA/GO Composite Fibers by Wet-spinning Assembly

A series of CS/PVA/GO solutions with GO ranging from 0 wt% to 1 wt%, 3 wt%, 5 wt% and 7 wt% were loaded into a 5 m*l* plastic syringe and injected into an absolute ethyl alcohol bath. After coagulation for 1 minute, the composite fibers were drawn out and collected on scroll and dried for 2 h at room temperature. Obtained fibers were labeled as CS/PVA, CS/PVA/GO 1, CS/PVA/GO 3, CS/PVA/GO 5 and CS/PVA/GO 7, respectively.

Characterization

The surface morphology of fibers with different ratio of graphene oxide were measured using a scanning electron microscope (SEM) (JEOL JSM-840, Japan).

Transmission electron microscopy (TEM) analysis was performed on composite fibers by a JEOL H-7650 TEM facility.

Fourier transform infrared spectra (FTIR) were used to obtain the information about the interactions among graphene oxide, chitosan and poly(vinyl alcohol). FTIR spectra were measured on a Nicolet 5700 FTIR spectrometer (Thermo Nicolet Corp., USA), which the wave number range was 4000-500 cm^{-1}.

Thermo gravimetric analysis (TGA) was recorded on a HTG-1 TGA instrument (Beijing Henven Instrument Factory, China). The temperature was programmed to increase from 80 to 700 °C at a ramp rate of 10 °C min^{-1} in nitrogen.

The powder X-ray diffraction (XRD) patterns were obtained with a DX-2700 X-ray diffractometer with Cu K_α radiation (40 kV, 40 mA). The recorded region of 2θ was 5-40 °, and the scanning speed was 2.0 ° min^{-1}.

The UV-blocking activities of the fibers, as assessed by UV protection factor (UPF), were recorded by UV spectrophotometer (UV1000F, Labsphere, USA). According to Australia/New Zealand standard AC/NZS 4399:1996, the UV protection factor (UPF) was calculated by equation (1) with the recorded data as follow:

$$UPF = \frac{\int_{290}^{400} E_\lambda \times S_\lambda \times d_\lambda}{\int_{290}^{400} E_\lambda \times S_\lambda \times T_\lambda \times d_\lambda} \quad (1)$$

where E_λ is the relative erythemal spectral effectiveness, S_λ is the solar UV spectral irradiance, T_λ is the spectral transmittance of the specimen (incoming light that passes through the specimen), d_λ is the wavelength increment (nm), and λ is the wavelength (nm).

Adsorption

Reactive red dyes were chosen as the model compound and the initial dye concentration (C_0) was 150 mg/*l*. The wavelength of maximum absorbance (λ_{max}) for reactive red dyes was 512 nm. The absorption experiment was carried out at room temperature, which was measured to be 20 ^{o}C.

To assess the absorption capacities of CS/PVA/GO fibers, fibers with different content of GO (0.1 g) and the dye solution (100 m*l*) were placed in 100 m*l* breakers. During the batch adsortption process, the residual dye concentration of each solution was determined by measuring its adsorbance using a UV-vis spectrophotometer (Mapada, UV-1800PC) at the predetermined time intervals. The equilibrium amount, q (mg/g), of composite fibers was calculated by equation (2):

$$q = \frac{(C_0 - C_t)V}{m} \tag{2}$$

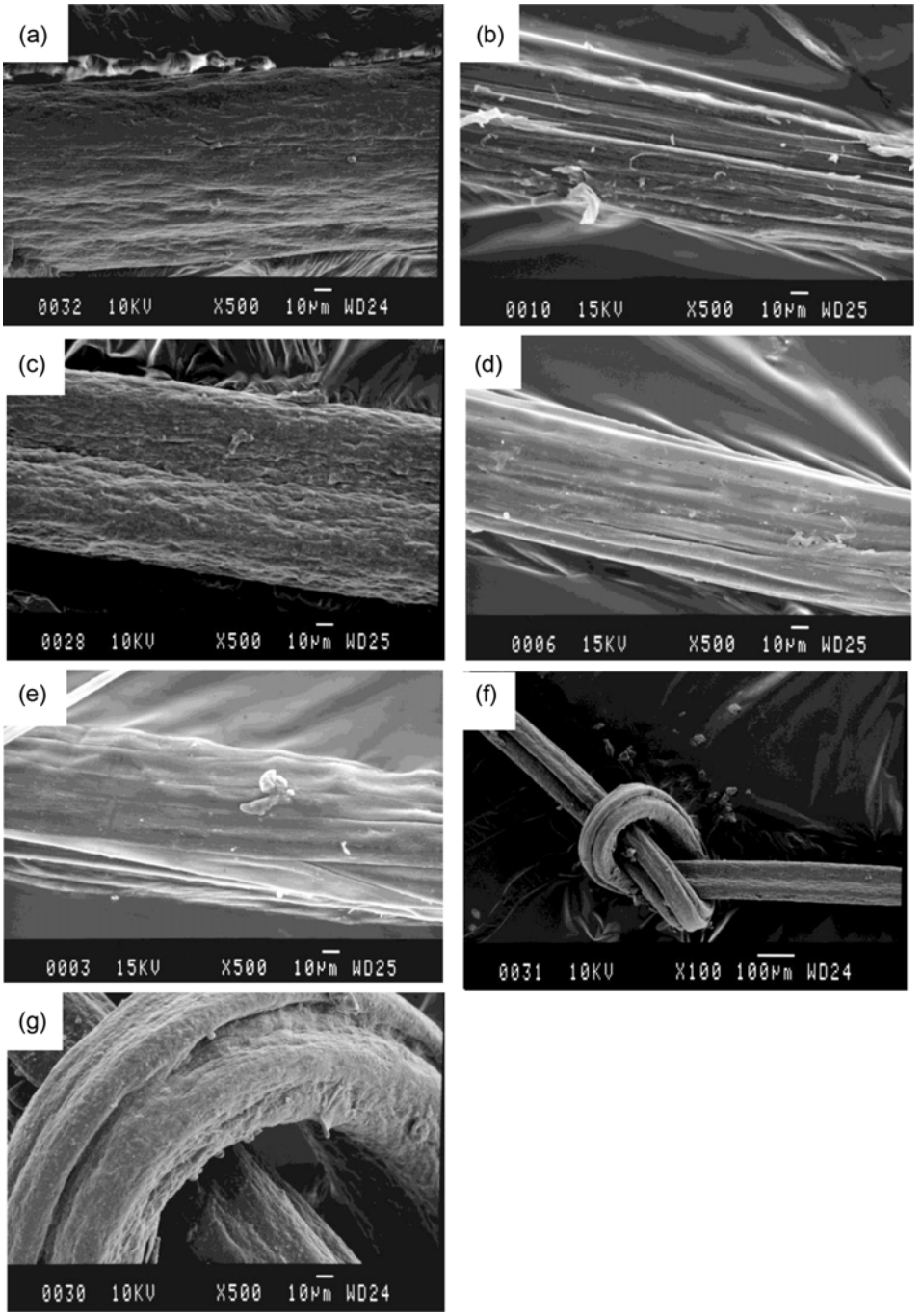

Figure 2. SEM micrographs of CS/PVA fibers (a), CS/PVA/GO 1 (b), CS/PVA/GO 3 (c), CS/PVA/GO 5 (d) and CS/PVA/GO 7 (e)-(g).

The percentage of rate (F) of reactive red dyes was analyzed from equation (3):

$$F = \frac{C_0 - C_t}{C_0} \times 100\% \quad (3)$$

where C_0 (mg/l) and C_t are the initial and transient concentrations of dye respectively, V is the volume of solution (L) and m is the mass of the fibers (g) [36].

In order to investigate the mechanism of adsorption, the effect of contact time (kinetic) on dye adsorption was studied in the time scale of 0-30 h. The transient concentration (C_t) of the dye was discussed by pseudo-first-order, pseudo-second-order equations [37].

A simple kinetic analysis of adsorption is the pseudo-first-order equation in the form:

$$C_t = C_0 - (C_0 - C_e) \times (1 - e^{-k_1 t}) \quad (4)$$

A pseudo-second-order equation based on adsorption equilibrium capacity may be expressed as equation (5):

$$C_t = C_0 - (C_0 - C_e) \times [1 - 1/(1 + k_2 t)] \quad (5)$$

where k_1 and k_2 (min^{-1}) are the rate constants for the pseudo-first-, pseudo-second-order kinetic models, respectively; C_0, C_t and C_e (mg/l) are the initial, transient and equilibrium concentrations of dye, respectively, in the aqueous solution.

Results and Discussion

Morphology and Structure of CS/PVA/GO Composite Fibers

All composite fibers were of remarkable performance in terms of uniform diameter, which was measured as around 80 μm in Figure 2. This is potentially because of good molecular interactions in spinning solutions that resulted in increasing polymer entanglement, uniform flow and fiber formation. Cylinder-shaped fibers with grooved surfaces were distinctly seen from Figure 2(a-e), especially that CS/PVA/GO 1 (Figure 2(b)) was observed to possess the most grooves while CS/PVA/GO 7 (Figure 2(e)) expressed the least ones. Such performance might be resulted from that excessive graphene oxide aggregated and had a negative effect on fiber surfaces. Apart from this, the fact that CS/PVA/GO fibers owned good flexibility was demonstrated in Figure 2(e-f).

In addition, the TEM image of CS/PVA/GO 1 as example was illustrated in Figure 3, GO platelets homogenously and freely embedded in the polymer matrix in the general view of CS/PVA/GO composite fibers in Figure 3(a), no obvious aggregation was detected in CS/PVA/GO 1 fiber. Furthermore, under the high-magnification in Figure 3(b), we found that almost GO acted as individual sheets.

The FTIR spectrum of GO in Figure 4(a) showed several characteristic absorbance bands centered at 3411 cm^{-1} (stretching vibration of hydroxyl groups), 1726 cm^{-1} (the stretching vibration of C=O from carboxylic groups), 1629 cm^{-1} (the stretching vibration of C=C), 1401 cm^{-1} (O-H deformation vibration), 1215 cm^{-1} (epoxy rings), 1052 cm^{-1} (C-OH bending) respectively, which was similar with previous references [38]. The result proved that GO was successfully synthesized from graphite. In the spectrum of CS, absorption peaks at 3421 cm^{-1}, 2884 cm^{-1}, 1653 cm^{-1}, 1602 cm^{-1} and 1382 cm^{-1} related to -OH stretching vibration, C-H stretching vibration, the C=O stretching vibration of -NHCO-, the N-H bending of -NH_2 and amide groups stretching vibration [39]. As shown in the spectrum of PVA, the broad and strong absorption at 3387 cm^{-1} corresponded to the symmetrical stretching vibration of -OH. And the peaks at 2927 cm^{-1} and 1095 cm^{-1} were due to -CH_2 and the stretching vibration of C-O, respectively [40].

The FTIR spectra of CS/PVA, CS/PVA/GO 1, CS/PVA/GO 3, CS/PVA/GO 5, CS/ PVA/GO 7 were shown in Figure 4(b).

Compared with CS and GO, both of peaks at 1602 cm^{-1} (-NH_2 absorbance vibration) and at 1726 cm^{-1} (C=O stretching vibration of carboxylic groups) disappeared in Figure 4(b). Moreover, the peak at 1726 cm^{-1} shifted to a lower wave-

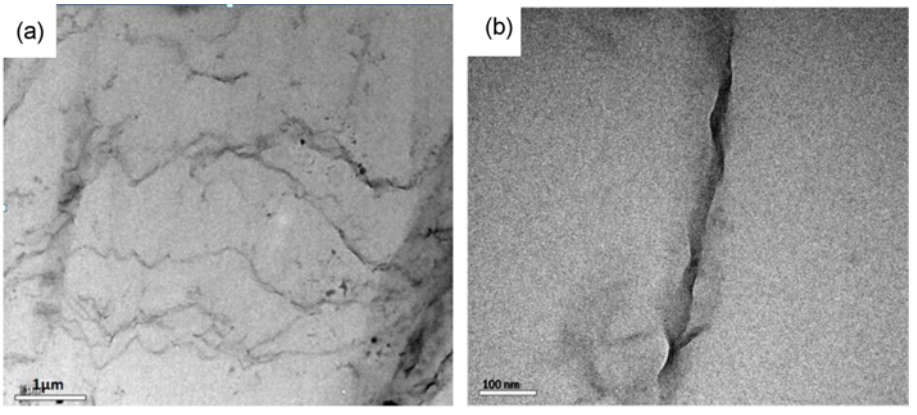

Figure 3. The TEM image of CS/PVA/GO 1 fibers.

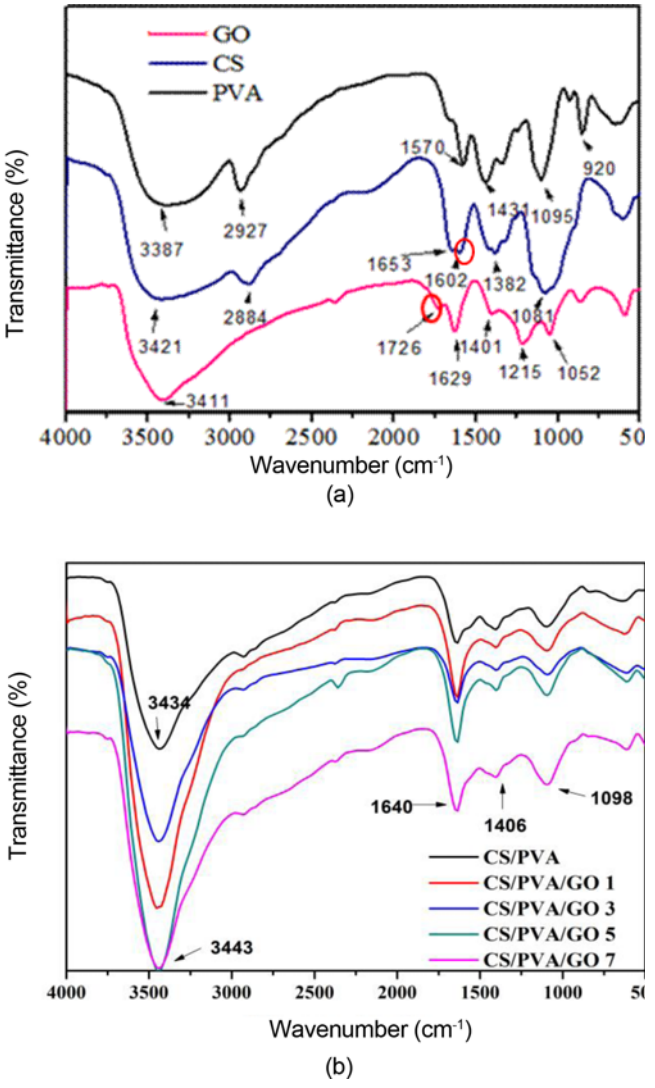

Figure 4. The FTIR spectra of pure GO, PVA and CS (a) and composite fibers (b).

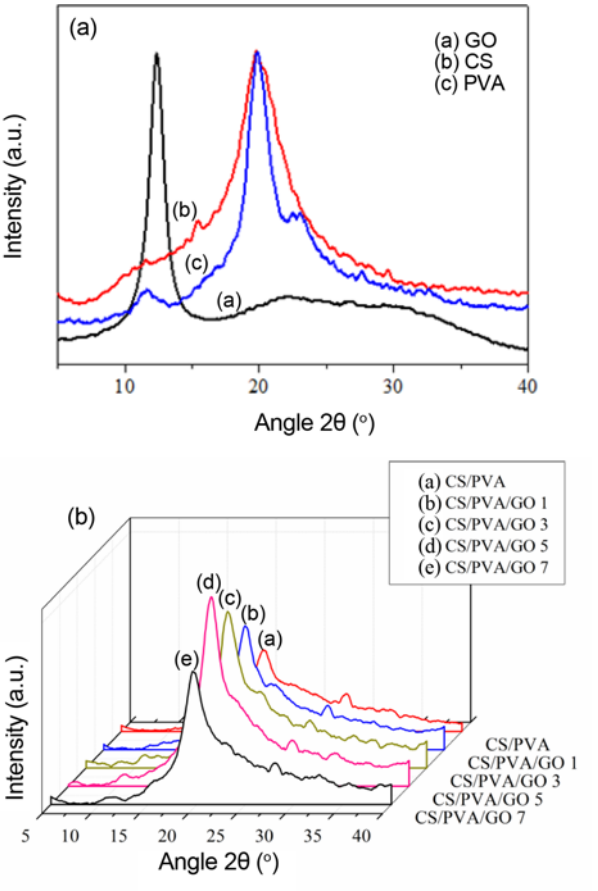

Figure 5. The X-ray diffraction patterns of GO, CS, PVA (a) and CS/PVA and CS/PVA/GO fibers with different content of GO (b).

number (1640 cm^{-1}). The reason was that the hydrogen bonding of CS and the oxygenated groups of GO generated the synergistic effect. And CS has a strong electrostatic interaction with GO sheets.

The XRD patterns of GO, CS and PVA in Figure 5(a) suggested that the characteristic diffraction peak of GO appeared at about 11°, corresponding to a d-spacing of 1.09 nm, according to Bragg equation [41]. Two typical peaks at 2θ=11.6° and 20° were observed in the X-ray diffraction pattern of CS [42], the peak at 2θ=11.6° reflected the hydrated crystalline structure while the broad peak 2θ=20° indicated the existence of an amorphous structure. And a characteristic peak at 19.8° was observed in the XRD pattern of pure PVA, revealing its crystal structure. In the CS/PVA fibers pattern, a weak peak was found at 19.8°, illustrating the existence of PVA lattice in composites. After different contents of GO were incorporated into the CS/PVA mixed matrix, there were the same peaks at 19.8° and 28° but the intensity of the peak at 19.8° increased by the content of GO growth. Compared with pure GO, the characteristic diffraction peak (11°) of GO disappeared in the patterns of CS/PVA/GO composite fibers shown in Figure 5(b). This disappearance demonstrated most of GO sheets were fully exfoliated in polymer matrices and the regular and periodic structure of graphene disappeared [39] or the characteristic diffraction peak was so weak so that it was overlapped by the peak of CS (11.6°). In conclusion, the incorporation of GO had a significant effect on the crystal structure of polymer matrix.

UV Protection Efficiency of CS/PVA/GO Fiber

The UV transmittance spectra of CS/PVA/GO fibers with different contents of GO were illustrated in Figure 6(a). In the range of the scanned wavelength (250-450 nm), the spectra demonstrated obvious distinction among the samples. Specially, the curves of CS/PVA expressed high UV transmittance implying that original CS/PVA had no effect on improving UV blocking of composite fibers. Once GO

was incorporated into composite fibers, the corresponding UV transmittance spectrums for CS/PVA/GO 1 reflected dramatic reduction. Choosing wavelength λ=450 nm as an example, UV transmittance of CS/PVA fibers reached up to 80.8 % while UV transmittance of CS/PVA/GO 1-7 fibers sharply dropped to 16.9 %, 3.4 %, 0.6 %, 0.4 % and 0.3 % respectively. Furthermore, it was seen from the UV transmittance spectrums (CS/PVA and CS/PVA/GO 1, 3, 5 and 7) that the function of UV blocking was apparently enhanced with the increasing GO contents (0-7 wt.%), demonstrating that UV blocking owed to graphene oxide to a remarkable extent. The result indicated that GO can effectively shield UV rays with low contents (1 wt.%).

The protection factor (UPF) values were used to estimate and define the efficiency of UV protection [5] as shown in Figure 6(b). According to the excellent protection UPF rating (50+) of Australian/New Zealand Standard AS/NZS 4399:1996, it was founded that all samples containing GO (CS/PVA/GO 1, 3, 5 and 7) dramatically took on more satisfactory UPF values than CS/PVA fibers. In order to assess the washing resistance of composite fibers, the contrast analysis was given between protection factor (UPF) values before and after washing 10 times. When the weight percentage of GO was only 1 %, the UPF value reached 60.36 before washing and 59.52 after washing. And when the content of GO was raised to 3 wt%, the UPF values sharply increased to 417.46 and 416 before and after washing, respectively. Finally, CS/PVA/GO5 and CS/PVA/GO 7 hardly allowed UV-rays to penetrate and UPF value added up to 500. By comparison, a conclusion could be drawn that the composite fibers had remarkably anti-ultraviolet capacity and good washing resistance. So it was predicted that the fabric that was made of CS/PVA/GO fibers could achieve the UV protection.

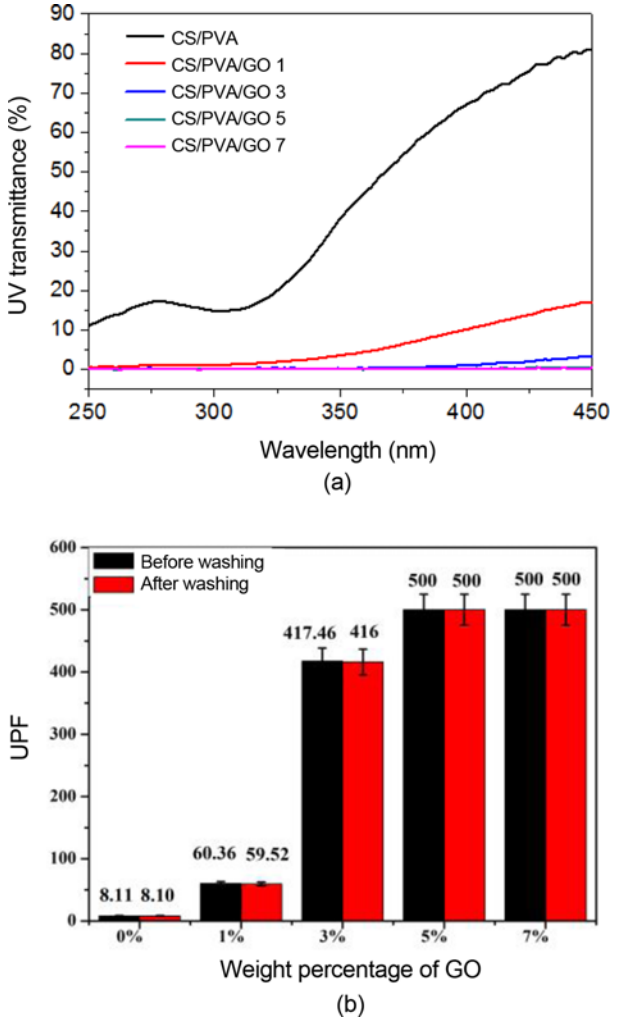

Figure 6. The UV transmittance spectrum (a) and UPF (b) of CS/PVA/GO fibers with different contents of GO.

Thermal Properties of CS/PVA/GO Composite Fibers

The thermogravimetric analyses (TGA) were used for describing the CS/PVA blends thermal behavior with GO loading. And the composite fibers with different content of GO were outlined in Figure 7. It was found that the decomposed residual weight of composite fibers was increased as the GO content increased. This may be attributed to the strong interaction between polymer matrix and graphene oxide.

It is generally accepted that reliable degradation temperature and kinetic parameters, including the initial decomposed temperature (IDT), the characteristic end-of-volatilization temperature (T_{A*}), the integral procedural decomposition temperature (IPDT) and so on, could be applied to assess the thermal stability of the blend system. Especially, IPDT suggested early by Doyle [43] could be discussed in a quantitative thermal analysis, whether decomposition was carried out in a single step or in several consecutive steps. According to Doyles's statement, the thermal stability factor

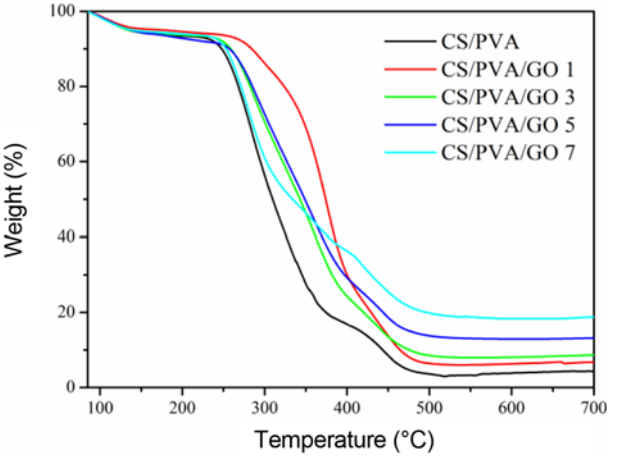

Figure 7. TGA curves of CS/PVA/GO fibers with different content of GO.

Table 1. IDT and thermal stability parameters for the composite fibers

Sample	IDT (°C)	A^*	T_{A^*} (°C)	K^*	A^*K^*	IPDT (°C)
CS/PVA	247	0.3920	326	1.2520	0.4907	392
CS/PVA/GO 1	284	0.4803	380	1.3411	0.6441	488
CS/PVA/GO 3	258	0.4476	360	1.2632	0.5654	438
CS/PVA/GO 5	257	0.4765	378	1.2270	0.5847	450
CS/PVA/GO 7	253	0.4973	391	1.1657	0.5797	447

for the blend system was determined by the TGA thermograms. And the IPDT was calculated by equation (6) as follows [44]:

$$IPDT(^{\circ}C) = A^*K^*(T_f - T_i) + T_i \quad (6)$$

where A^* is the area ratio of total experimental curve divided by total TGA thermogram, K^* the coefficient of A^*, T_i the intial experimental temperature (85 °C), and T_f the final experimental temperature (700 °C).

The values of IDT and IPDT parameters (A^* and K^*) was listed in Table 1. The results of IDT clearly indicated that the thermal stability of composite fibers could be effectively enhanced by grafting GO, comparing CS/PVA with CS/PVA/GO 1-7. Even so, GO was not the more the better. As expected, the IDT was somewhat decreased from 284 °C to 258 °C as the GO content increased from 1 wt.% to 7 wt.%. The result implied that low content of GO could well dispersed and form intermolecular interaction (hydrogen bonding) and strong electrostatic interaction, due to amino and hydroxyl groups and so on. However, higher content of GO (3-7 wt.%) maybe result in aggregation and redundant GO existed as the impurities so that it was possibly to have negative effect on improvement of thermal property. At the same time, The IPDT is a reproducible datum having practical significance as an integrated half-volatilization temperature. Moreover, the values of IPDT reported a result similar to those of IDT, which 1 wt.% GO revealed the highest temperature (488 °C) among them, or put it other way, the most remarkable thermal stability. In addition, Table 2 showed that CS/PVA/GO 1 (1 wt.% GO) always remained the same weights (95 % and 50 % respectively) at a higher temperature than other samples.

But all above, low content of GO (1 wt.%) played a dramatic role on enhancing the thermal stability of composite fibers.

Adsorptive Properties of CS/PVA/GO Composite Fibers

As shown in Figure 8, the color of dyes became gradually light in order of (b) CS/PVA/GO 1, (a) CS/PVA, (c) CS/PVA/GO 3, (d) CS/PVA/GO 5 and (e) CS/PVA/GO 7. It was easily found that CS/PVA/GO 1 fiber (1 wt.%) was the best absorbent (407 mg/g), but the adsorptive capacity of fibers was on the decline with the increasing GO contents (3, 5 and 7 wt.%), which was even not good as CS/PVA (0 wt.%). The reason was probably that the adsorption mechanism and the dispersed state of GO changed in composite fibers. As to the adsorption mechanism of GO, there exist a π-π interaction and the electrostatic repulsion between the reactive red dye and GO sheets. If the π-π interaction dominates, the resultant fibers show high adsorption capacity for reactive red and vice versa. The content of GO is lower (1 wt.%) in CS/PVA/GO 1, once GO mixed with CS, one part of the negative charges on GO sheets might be neutralized with the positive charges in CS, so the π-π interaction between GO and reactive red in CS/PVA/GO 1 was deemed as the dominated mechanism of the enhanced adsorption capacity. However, with the increasing GO in CS/PVA/GO 3-7, the amount of

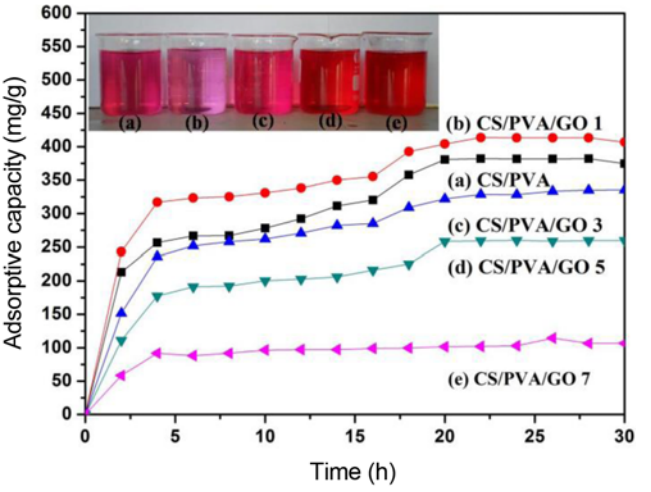

Figure 8. The adsorptive capacity of fibers with different contents of GO; (a) CS/PVA, (b) CS/PVA/GO 1, (c) CS/PVA/GO 3, (d) CS/PVA/GO 5, and (e) CS/PVA/GO 7.

Table 2. The temperature of different weight (%) in TGA curves

Weight (%)	CS/PVA (°C)	CS/PVA/GO 1 (°C)	CS/PVA/GO 3 (°C)	CS/PVA/GO 5 (°C)	CS/PVA/GO 7 (°C)
95	134	177	134	137	140
50	309	374	342	348	334

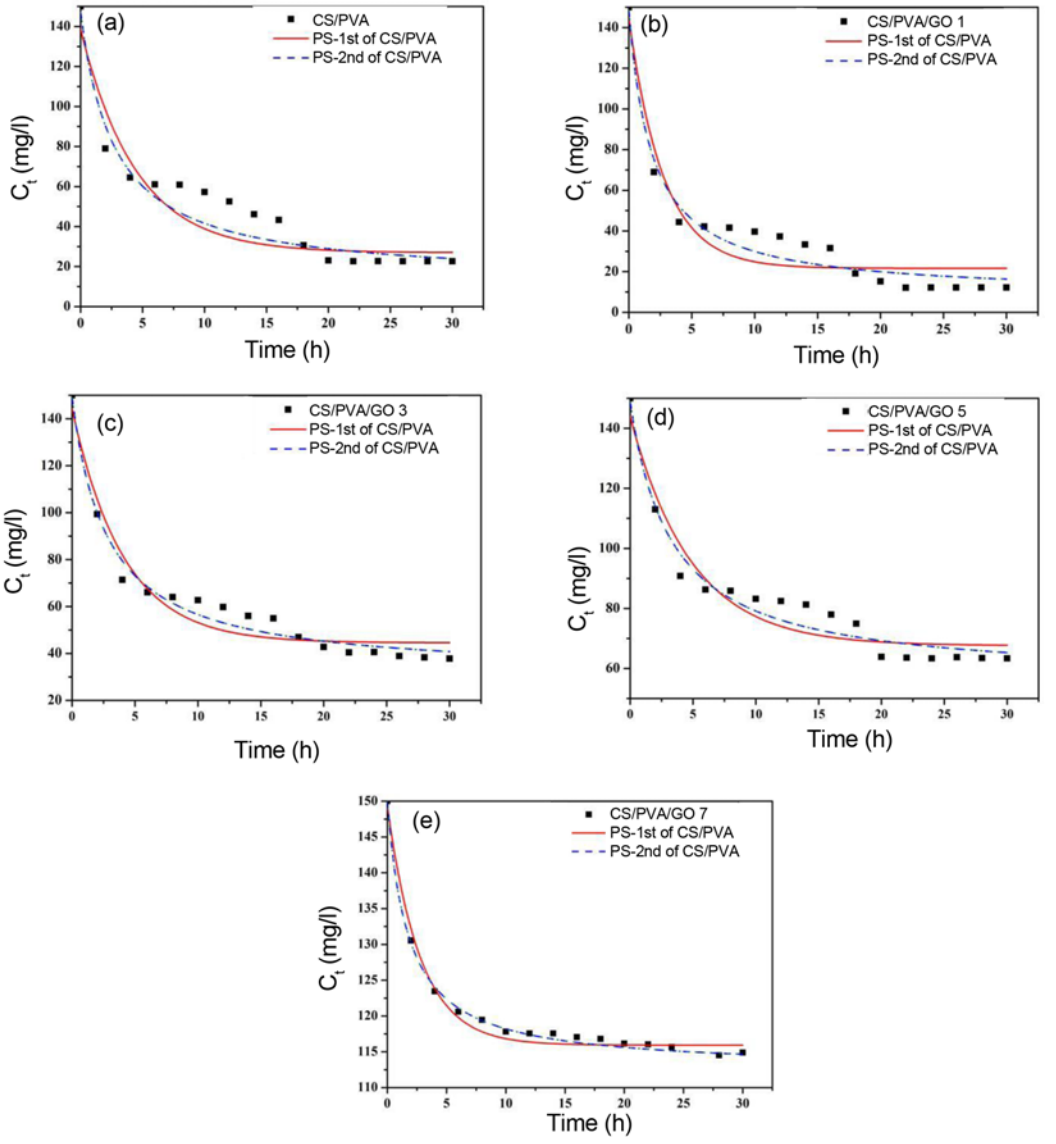

Figure 9. Effect of contact time on adsorption of dye onto composite fibers; (a) CS/PVA, (b) CS/PVA/GO 1, (c) CS/PVA/GO 3, (d) CS/PVA/GO 5, and (e) CS/PVA/GO 7.

negative charge of GO increased, the π-π interaction between GO and reactive red might be gradually replaced by the electrostatic repulsion between these two anionic materials. Therefore, the adsorption capacity for dyes was dramatically attenuated. In addition, the dispersed state of GO might also be concerned, GO was mostly dispersed as the single layer in CS/PVA/GO 1 according to the TEM results. Once the content of GO exceeded a certain value (1 wt.%), GO layers were accumulated and formed multiple layers so that a considerable part of their surface area were lost. The surface area was a key factor for an absorbent, so excessive GO limited the absorptive capacity for dyes. In a word, CS/PVA/GO fibers could be applied to the water purification and easier to collect from water than powders or liquid.

Figure 9 showed the effect of contact time on adsorption of dye onto composite fibers. At the initial stage (0-4 h), the fast dye adsorption was found due to an external surface diffusion. The reason was that a large number of surface sites were available for dye molecules. However, the adsorption rate became slower at the intermediary stage (4-20 h) until the equilibrium state reached at the last stage (20-30 h). The slower adsorption was due to two facts: a small quantity of sites remained in the surface of fibers; the repulsion force between the solute molecules of solid and bulk phases made it harder for dye molecules to latch onto the fiber surface. Finally, the adsorption with increasing time reached the dynamic balance. Table 3 reported the kinetic parameters resulting from fits to pseudo-first-order, pseudo-second-

Table 3. Kinetic constants for the adsorption of dye onto composite fibers

Adsorbent	Pseudo-first-order		Pseudo-second-order	
	k_1 (min^{-1})	R^2	k_2 (min^{-1})	R^2
CS/PVA	0.223	0.926	0.366	0.971
CS/PVA/GO 1	0.364	0.899	0.546	0.955
CS/PVA/GO 3	0.245	0.934	0.356	0.973
CS/PVA/GO 5	0.206	0.911	0.301	0.953
CS/PVA/GO 7	0.360	0.969	0.564	0.987

order equations to the experimental data. From Table 3, it could be seen that non-linear fits were generally observed for all fibers, implying that sorption reaction can be approximated to be of the pseudo-first order kinetics. Correlation coefficients were found to be between 0.899 and 0.969, which means that there was a good agreement but not a perfect one. It may be attributed to the fact that the pseudo-first-order equation is generally applicable over the initial stage of the adsorption processes, but it doesn't fit well to the whole range of contact time in many cases [45]. According to the correlation coefficients (R^2), Better fits were obtained with pseudo-second-order model. The largest correlation coefficient in this case was 0.987, which was much better than the pseudo-first-order model. It made sense to discuss the physical significance of the so-called pseudo-first- and pseudo-second-order equations in current study [37]. In conclusion, the kinetics was dominated by the rate of surface reactions at the initial stage of adsorption while intraparticle diffusion worked approaching to equilibrium phase.

Conclusion

In conclusion, the multifunctional chitosan (CS)/poly(vinyl alcohol) (PVA)/graphene oxide (GO) composite fibers were obtained by wet-spinning route. In the process, ethanol was used as coagulating bath. And the resultant fibers achieved remarkable anti-ultraviolet capability, adsorptivity and thermal property. Moreover, the more content of GO in composite fibers was not better. As the functional material, GO can express excellent properties at a threshold value of 1 wt.%, at which it showed the most excellent thermal stability and the highest absorptive capacity of 407 mg/g among all the resultant fibers and its transmittance decreased to 3.4 %, corresponding to UPF as 417.46. Due to these outstanding properties, CS/PVA/GO composite fibers will have a bright future in applications, for instance, in textile and wastewater treatment.

Acknowledgment

Financial support of this work was provided by Natural Science Foundation of China via grant No. 51273097 and 51306095, China Postdoctoral Science Foundation via grant No. 2014M561887 and 2015T80697 and Taishan scholars construction engineering of Shandong province.

References

1. Z. Xu, H. Sun, X. Zhao, and C. Gao, *Adv. Mater.*, **25**, 188 (2013).
2. J. Liang, Y. Huang, L. Zhang, Y. Wang, Y. Ma, T. Guo, and Y. Chen, *Adv. Funct. Mater.*, **19**, 2297 (2009).
3. Y. Y. Qi, Z. X. Tai, D. F. Sun, J. T. Chen, H. B. Ma, X. B. Yan, B. Liu, and Q. J. Xue, *J. Appl. Polym. Sci.*, **127**, 1885 (2013).
4. Y. Xu, W. Hong, H. Bai, C. Li, and G. Shi, *Carbon*, **47**, 3538 (2009).
5. L. Qu, M. Tian, X. Hu, Y. Wang, S. Zhu, X. Guo, G. Han, X. Zhang, K. Sun, and X. Tang, *Carbon*, **80**, 565 (2014).
6. W. Ma, J. Li, and X. Zhao, *J. Mater. Sci.*, **48**, 5287 (2013).
7. J. Duan, S. Shao, L. Wang, P. Jiang, and B. Liu, *Iran. Polym. J.*, **21**, 109 (2012).
8. S. Vadukumpully, J. Paul, N. Mahanta, and S. Valiyaveettil, *Carbon*, **49**, 198 (2011).
9. X. Zhao, Z. Liu, W. Yan, Y. Wu, X. Zhang, Y. Chen, and J. Tian, *Appl. Phys. Lett.*, **98**, 121905 (2011).
10. Y. Li, T. Yang, T. Yu, L. Zheng, and K. Liao, *J. Mater. Chem.*, **21**, 10844 (2011).
11. K. Shin, J. Hong, S. Lee, and J. Jang, *J. Mater. Chem.*, **22**, 7871 (2012).
12. Y. Huang, Y. Qin, Y. Zhou, H. Niu, Z. Yu, and J. Dong, *Chem. Mater.*, **22**, 4096 (2010).
13. Y. S. Yun, Y. H. Bae, D. H. Kim, J. Y. Lee, I. Chin, and H. Jin, *Carbon*, **49**, 3553 (2011).
14. J. Xu, Y. Liang, H. Huang, G. Zhong, J. Lei, C. Chen, and Z. Li, *J. Polym. Res.*, **19** (2012).
15. Y. Chen, Y. Qi, Z. Tai, X. Yan, F. Zhu, and Q. Xue, *Eur. Polym. J.*, **48**, 1026 (2012).
16. A. U. Chaudhry and V. Mittal, *Polym. Eng. Sci.*, **53**, 78 (2013).
17. K. Deshmukh, S. M. Khatake, and G. M. Joshi, *J. Polym. Res.*, **20**, 1 (2013).
18. H. J. Salavagione and G. Martínez, *Macromolecules*, **44**, 2685 (2011).
19. J. Jang, M. Kim, H. Jeong, and C. Shin, *Compos. Sci. Technol.*, **69**, 186 (2009).
20. D. Cai, K. Yusoh, and M. Song, *Nanotechnology*, **20**, 85712 (2009).
21. N. Yousefi, M. M. Gudarzi, Q. Zheng, S. H. Aboutalebi, F. Sharif, and J. Kim, *J. Mater. Chem.*, **22**, 12709 (2012).
22. D. Han, L. Yan, W. Chen, W. Li, and P. R. Bangal, *Carbohydr. Polym.*, **83**, 966 (2011).
23. D. Han, L. Yan, W. Chen, and W. Li, *Carbohydr. Polym.*, **83**, 653 (2011).
24. X. Yang, Y. Tu, L. Li, S. Shang, and X. Tao, *ACS Appl. Mater. Int.*, **2**, 1707 (2010).

25. G. Crini, *Prog. Polym. Sci.*, **30**, 38 (2005).
26. L. Fan, C. Luo, M. Sun, X. Li, F. Lu, and H. Qiu, *Bioresource Technol.*, **114**, 703 (2012).
27. L. Liu, C. Li, C. Bao, Q. Jia, P. Xiao, X. Liu, and Q. Zhang, *Talanta*, **93**, 350 (2012).
28. L. Fan, C. Luo, X. Li, F. Lu, H. Qiu, and M. Sun, *J. Hazard. Mater.*, **215**, 272 (2012).
29. Y. Chen, L. Chen, H. Bai, and L. Li, *J. Mater. Chem. A*, **1**, 1992 (2013).
30. L. Qu, X. Guo, M. Tian, and A. Lu, *Fiber. Polym.*, **15**, 1357 (2014).
31. A. Aytimur and İ. Uslu, *Polym.-Plast. Technol. Eng.*, **53**, 655 (2014).
32. H. Bai, C. Li, X. Wang, and G. Shi, *Chem. Commun.*, **46**, 2376 (2010).
33. H. M. Kim, J. K. Lee, and H. S. Lee, *Thin Solid Films*, **519**, 7766 (2011).
34. W. S. Hummers Jr and R. E. Offeman, *J. Am. Chem. Soc*., **80**, 1339 (1958).
35. M. Tian, L. Qu, X. Zhang, K. Zhang, S. Zhu, X. Guo, G. Han, X. Tang, and Y. Sun, *Carbohydr. Polym.*, **111**, 456 (2014).
36. K. Azlan, W. N. Wan Saime, and L. Lai Ken, *J. Environ. Sci.*, **21**, 296 (2009).
37. N. A. Travlou, G. Z. Kyzas, N. K. Lazaridis, and E. A. Deliyanni, *Langmuir*, **29**, 1657 (2013).
38. J. Shen, M. Shi, B. Yan, H. Ma, N. Li, and M. Ye, *Nano Res.*, **4**, 795 (2011).
39. X. Yang, Y. Tu, L. Li, S. Shang, and X. Tao, *ACS Appl. Mater. Int.*, **2**, 1707 (2010).
40. C. Bao, Y. Guo, L. Song, and Y. Hu, *J. Mater. Chem.*, **21**, 13942 (2011).
41. L. Liu, C. Li, C. Bao, Q. Jia, P. Xiao, X. Liu, and Q. Zhang, *Talanta*, **93**, 350 (2012).
42. L. Qu, X. Guo, M. Tian, and A. Lu, *Fiber. Polym.*, **15**, 1357 (2014).
43. C. D. Doyle, *Anal. Chem.*, **33**, 77 (1961).
44. S. Park, H. Kim, H. Lee, and D. Suh, *Macromolecules*, **34**, 7573 (2001).
45. M. S. Chiou and H. Y. Li, *J. Hazard. Mater.*, **93**, 233 (2002).